Ocean Sci. Discuss., 12, 2395–2421, 2015
www.ocean-sci-discuss.net/12/2395/2015/
doi:10.5194/osd-12-2395-2015

Ocean Science
Discussions
Open Access

Effects of lateral processes on the seasonal water stratification of the Gulf of Finland: 3-D NEMO-based model study

R. E. Vankevich[1,2], E. V. Sofina[1,2], T. E. Eremina[1], A. V. Ryabchenko[2], M. S. Molchanov[1], and A. V. Isaev[1,2]

[1]Russian State Hydrometeorological University, Saint-Petersburg, Russia
[2]The St.-Petersburg Branch of the P. P. Shirshov Institute of Oceanology of the Russian Academy of Sciences, Saint-Petersburg, Russia

Received: 27 August 2015 – Accepted: 9 September 2015 – Published: 12 October 2015

Correspondence to: R. E. Vankevich (rvankevich@mail.ru)

Published by Copernicus Publications on behalf of the European Geosciences Union.

Abstract

This paper tries to fill the gaps in knowledge of processes affecting the seasonal water stratification in the Gulf of Finland (GOF). We used state-of-the-art modeling framework NEMO aimed for oceanographic research, operational oceanography, seasonal forecasting and climate studies to build an eddy resolving model of the GOF. To evaluate the model skill and performance two different solutions where obtained on 0.5 km eddy resolving and commonly used 2 km grids for one year simulation. We also explore the efficacy of nonhydrostatic effect (convection) parameterizations available in NEMO for coastal application. It is found that the solutions resolving sub-mesoscales have a more complex mixed layer structure in the regions of GOF directly affected by the upwelling/downwelling and intrusions from the open Baltic Sea. Presented model estimations of the upper mixed layer depth are in a good agreement with in situ CTD data. A number of model sensitivity tests to the vertical mixing parameterization confirm the model robustness.

1 Introduction

The Gulf of Finland (GOF) is a 400 km long and 48–135 km wide sub-basin of the Baltic Sea with a mean depth of 37 m and complex bathymetry. The large fresh input from Neva River significantly affects the stratification and forms the strong salinity gradient from east to west and from north to south. Sea-surface salinity decreases from 5 to 6.5 ‰ in the western GOF to about 0–3 ‰ in the easternmost part of the Gulf where the role of the Neva River is most pronounced (Alenius et al., 1998). In the western GOF, a quasi-permanent halocline is located at a depth of 60–80 m. Salinity in that area can reach values as high as 8–10 ‰ near the sea bed due to the advection of saltier water masses from the Baltic Proper.

The vertical stratification in the GOF as well as in the Baltic Sea is unusual (the thermocline and halocline are usually separated) with a pronounced and relatively stable

OSD
12, 2395–2421, 2015

Effects of lateral processes on the seasonal water stratification of the Gulf of Finland

R. E. Vankevich et al.

halocline, whereas the temperature is largely controlled by the seasonal variability of the surface heat fluxes (see e.g. Hankimo, 1964). During the summer season the water column in the deeper areas of the GOF consists of the three layers – the upper mixed layer (UML), the cold intermediate layer (CIL) and a saltier and slightly warmer near-bottom layer, separated by two pycnoclines – the thermocline at the depths of 10–20 m and the permanent halocline at the depths of 60–70 m. A seasonal thermocline starts to develop in May. The surface mixed layer reaches a maximum depth of 15–20 m by midsummer and an erosion of the thermocline starts in late August due to wind mixing and thermal convection. The bottom salinity also shows significant spatiotemporal variability due to irregular saline water intrusions from the Baltic Proper, as well as from changes in river runoff and the precipitation-evaporation balance. There is no permanent halocline in the eastern GOF, where salinity increases approximately linearly with depth (Nekrasov and Lebedeva, 2002; Alenius et al., 2003).

The simulations of the vertical stratification using 3-D numerical models are not so reliable yet (Myrberg et al., 2010). This study shows that the best existing 3-D scientific circulation models are able to simulate the major features of the hydro-physical fields of the GOF. For example, the hind-cast mean temperatures differ from observations by less than 1–2 °C and the mean error in salinity is less than 1 ‰. Most of the remaining difficulties are connected with problems in adequately representing the dynamics of the mixed layer. The loss of accuracy is most notable in the simulation of the depth and the sharpness of the corresponding thermo- and haloclines. Despite the application of sophisticated turbulent closure schemes and different schemes for vertical mixing, none of the models, analyzed in Myrberg et al. (2010), were able to accurately simulate the vertical profiles of temperature and salinity. Latest experiments with turbulence parameterizations of 3-D hydrodynamic model COHERENS presented in Tuomi et al. (2013) show that model still underestimate the thermocline depth. Also the sensitivity of the modelled thermocline depth to the accuracy of the meteorological forcing was studied by increasing the forcing wind speed to better match the measured values of wind speed in the central GOF. The sensitivity test showed that an increase in the wind

OSD
12, 2395–2421, 2015

speed only slightly improved the performance of the turbulence parameterizations in modelling the thermocline depth.

However, a number of studies have reported important effects of the vertical thermohaline structure on the characteristics and processes in the marine ecosystems of the GOF, such as phytoplankton species composition (Rantajarvi et al., 1998) and subsurface maxima of phytoplankton biomass (Lips et al., 2010), cyanobacteria blooms (Lips et al., 2008), distribution of pelagic fish (Stepputtis et al., 2011), macrozoobenthos abundance (Laine et al., 2007) and oxygen concentrations in the near bottom layer (Maximov, 2006).

Summarizing all written above, prediction of the thermohaline structure is a complex problem for the GOF. The spatial variability of thermohaline structure encompass a wide range of physical processes at different scales, some of which are still poorly understood (Soomere et al., 2008, 2009). For example, we believe that the local stratification depends very strongly a on the across GOF movements of water masses and sub-mesoscale eddies generated by baroclinic instability of fronts in upper layers of the sea play an important role in heterogeneity of spatial distribution of parameters (temperature, nutrients, phytoplankton) but also they can act to re-stratify the UML ocean, as described in Gent and McWilliams (1990).

In the ocean, submesoscales are scales of motion equal or less than the Rossby radius of deformation but large enough to be influenced by planetary rotation (Thomas et al., 2007). Recent studies showed that increasing the horizontal resolution of the model up to 0.5 km (for the GOF Rossby radius aprox. 2–4 km) enables models to resolve submesoscale eddies. As a result, surface currents and temperatures show highly detailed patterns that qualitatively match well with the expected features (Sokolov, 2013; Zhurbas et al., 2008). However, there was no yet considered the influence of eddy motions and across Gulf movements of water masses on vertical re-stratification of the upper mixed layer of the GOF.

The motivations behind this study are:

OSD
12, 2395–2421, 2015

– to provide an insight into the submesoscale and basin-scale processes in the GOF. We are interested, in particular, in learning how lateral advection processes contribute to the thermocline variations.

– to assess the impact of horizontal grid resolution on the representation of vertical stratification.

2 Approach

Traditional point of view is that the eddy diffusion dominates in the horizontal direction and in the vertical direction mixing due to eddies is limited, and small scale processes such as turbulence provide the majority of mixing. Based on this idea most commonly 1-D approach is used to set up vertical mixing by tuning a turbulent scheme. For the GOF as an enclosed basin with complex bathymetry and strong stratification mixed layer dynamics can be strongly affected by lateral advective processes. To investigate this phenomenon we present a state-of-the art three-dimensional model of the GOF with high vertical and two different horizontal resolutions. Shelf sea modelling is characterized by a demand for a many different configurations to meet multiple science and user needs. NEMO gives the capability to rapidly configure shelf sea models using appropriate high resolutions and parameterizations on the representation of coastal dynamics.

2.1 General model set-up

Our study is based on a 3-D thermo-hydrodynamic model build on the NEMO (Nucleus for European Modelling of the Ocean) code initially designed for the open ocean and adopted by our team for the GOF (NEMO GOF). The NEMO is a 3-D hydrostatic, baroclinic primitive equation model toolkit laid out horizontally on the Arakawa C-grid (Madec et al., 1998; Madec, 2012). The NEMO is developing in a framework of a community European institutes and benefit of the recent scientific and technical develop-

OSD
12, 2395–2421, 2015

ments implemented in most ocean modeling platforms. The NEMO implementation for the GOF uses the TVD advection scheme in the horizontal direction, the piecewise parabolic method (PPM) in the vertical direction (Liu and Holt, 2010), the non-linear variable volume (VVL) scheme for the free surface. In the horizontal plane, the model uses the standard Jacobean formulation for the pressure gradient, the viscosity and diffusivity formulation with a constant coefficient for momentum and tracer diffusion. The horizontal viscosity and diffusivity operators are rotated to be aligned with the density iso-surfaces to accurately reproduce density flows.

In this paper, we used gridded bathymetric data set with a resolution of 0.25 nm for the GOF (Andrejev, 2010). Choosing different grid resolutions of the model is formally equivalent to the choice of an appropriate averaging operator (low-pass filtering at the grid step) and an approach to estimate the contribution of smaller scales to the general motion. To assess the impact of submesoscale motion on the vertical stratification, two configurations of NEMO GOF were generated by utilizing different horizontal and the same vertical resolution of 1 m. Both configurations have 94 vertical levels, but 1 min zonal and 2 min meridional resolution ($\sim$ 2 km) in a standard configuration and 0.25 min zonal and 0.5 min meridional resolution ($\sim$ 0.5 km) in a finer resolution configuration. The parameters of configurations were kept as identical as possible. The main exception is the coefficients of horizontal diffusivity and viscosity which were set to the minimum values guaranteeing the numerical stability.

Numerical experiments were started from rest and initialized with temperature and salinity from operational model of Baltic Sea HIROMB (Funkquist, 2001). The computational domain covers entire GOF with open boundary set at 23E longitude, boundary conditions being taken also from HIROMB. The model was forced by the surface forcing dataset HIRLAM (http://hirlam.org) (using the CORE bulk forcing algorithm) and climatic rivers runoff (Stalnacke et al., 1999).

OSD
12, 2395–2421, 2015

2.2 Parameterization of convective flows

One of the possible mechanisms by which the lateral motion affects the stratification is a shear-induced convection: situation in which heavy water may be advected on top of lighter water. This mechanism has been observed, e.g. in the bottom boundary layer of lakes (Lorke et al., 2005) and on the continental shelf (Rippeth et al., 2001). Evidently, the shear-induced convection can take place throughout the water column, for example, during upwelling. In nature, convective processes quickly re-establish the static stability of the water column (Umlauf, 2005). These processes have been removed from the model via the hydrostatic assumption so they must be parameterized.

To reproduce convective mixing by turbulent closure scheme NEMO offers: (1) a computationally efficient solution "TKE scheme" in combination with convective adjustment procedures (a non-penetrative convective adjustment or an enhanced vertical diffusion) and (2) physically more accurate the "GLS scheme".

The "TKE scheme" is a turbulence closure scheme proposed by Bougeault and Lacarrére (1989) originally developed to a model of the atmospheric boundary layer. In the Mellor and Yamada (1974) hierarchy it is a 1.5-level closure and consists of a prognostic closure for the turbulent kinetic energy (TKE) and an algebraic formulation for the mixing length scale. The time evolution of TKE is the result of the production of TKE through vertical shear, its suppression through stratification, its vertical diffusion, and its dissipation of Kolmogorov (1942) type:

$$\frac{\partial \overline{e}}{\partial t} = \frac{K_m}{e_3^2}\left[\left(\frac{\partial u}{\partial k}\right)^2 + \left(\frac{\partial v}{\partial k}\right)^2\right] - K_\rho N^2 + \frac{1}{e_3}\frac{\partial}{\partial k}\left[\frac{K_e}{e_3}\frac{\partial \overline{e}}{\partial k}\right] - C_\varepsilon \frac{\overline{e}^{3/2}}{l_\varepsilon}, \tag{1}$$

$$K_m = C_k l_k \sqrt{\overline{e}}, \tag{2}$$

$$K_\rho = K_m / P_{\mathrm{rt}} \tag{3}$$

where N is the local buoyancy frequency, l_c and l_k are the dissipation and mixing length scales, u and v are the horizontal velocity components, k is the layer number, $e_3 = 1$ m

Discussion Paper | Discussion Paper | Discussion Paper | Discussion Paper |
OSD
12, 2395–2421, 2015
Effects of lateral processes on the seasonal water stratification of the Gulf of Finland
R. E. Vankevich et al.

is the vertical scale factor, P_{rt} is the Prandtl number, K_m and K_ρ are the vertical eddy viscosity and diffusivity coefficients. The parameter C_k is known as a stability function and is defined as a constant in the TKE scheme. The constants $C_k = 0.1$ and $C_\varepsilon = 0.7$ are designed to deal with vertical mixing at any depth (Gaspar et al., 1990). K_e is the eddy diffusivity coefficient for the TKE. In NEMO $K_\mathrm{e} = K_m$.

For computational efficiency, the original formulation of the turbulent length scales proposed by Gaspar et al. (1990) has been simplified to the following first order approximation

$$l_k = l_\varepsilon = \sqrt{2\overline{e}}/N. \quad (4)$$

This simplification valid in a stable stratified region with constant values of the buoyancy frequency has two major drawbacks: it makes no sense for locally unstable stratification and the computation no longer uses all the information contained in the vertical density profile. To overcome these drawbacks, NEMO TKE implementation adds an extra assumption concerning the vertical gradient of the computed length scale. So, the length scales are first evaluated as in Eq. (4) and then bounded such that:

$$\frac{1}{e_3}\left|\frac{\partial l}{\partial k}\right| \leq 1, \text{ with } l = l_k = l_\varepsilon \quad (5)$$

In order to impose the constraint Eq. (5), NEMO introduces two additional length scales: l_{up} and l_{dwn}. The length scales l_{up} and l_{dwn} are respectively the upward and downward distances to which a fluid parcel is able to travel from current z level k, converting its TKE into the potential energy by doing work against the stratification, and they can be evaluated as:

$$l_{\mathrm{up}}^{(k)} = \min\left(l^{(k)}, l_{\mathrm{up}}^{(k+1)} + e_3^{(k)}\right) \text{ from } k = 1 \text{ to } nk \quad (6)$$

$$l_{\mathrm{dwn}}^{(k)} = \min(l^{(k)} l_{\mathrm{dwn}}^{(k-1)} + e_3^{(k-1)}) \text{ from } k = nk \text{ to } 1, \quad (7)$$

OSD
12, 2395–2421, 2015
Effects of lateral processes on the seasonal water stratification of the Gulf of Finland
R. E. Vankevich et al.

where nk is the number of level in vertical, $l^{(k)}$ is computed using Eq. (4), i.e.

$$l^{(k)} = \sqrt{2\overline{e}^{(k)}/N^{2(k)}}. \tag{8}$$

Finally,

$$l_k = l_\varepsilon = \min(l_{up} l_{dwn}). \tag{9}$$

The Generic Length Scale (GLS) scheme is formally equivalent to the TKE scheme, excepting using: (1) a prognostic equation for the generic length scale ϕ and (2) expressions for the complex stability functions instead constants. We used $k-\varepsilon$ turbulent closure scheme (Rodi, 1987) with its $\phi = C^3_{0\mu}\overline{e}^{3/2}l^{-1}$, where $C_{0\mu}$ is a constant depending on the choice of the stability function (Galperin et al., 1988; Kantha and Clayson, 1994).

This prognostic length scale is valid for convective situations and arbitrary increase diffusivity to represent convection (Umlauf and Burchard, 2003, 2005):

$$\frac{\partial \phi}{\partial t} = \frac{\phi}{\overline{e}}\left\{\frac{C_1 K_m}{\sigma_\phi e_3}\left[\left(\frac{\partial u}{\partial k}\right)^2 + \left(\frac{\partial v}{\partial k}\right)^2\right] - C_3 K_\rho N^2 - C_2 \varepsilon\right\} + \frac{1}{e_3}\frac{\partial}{\partial k}\left[\frac{K_m}{e_3}\frac{\partial \phi}{\partial k}\right] \tag{10}$$

$$K_m = C_\mu \sqrt{\overline{e}} l, \tag{11}$$

$$K_\rho = C_{\mu'} \sqrt{\overline{e}} l, \tag{12}$$

$$\varepsilon = C_{0\mu}\overline{e}^{3/2} l^{-1}, \tag{13}$$

Here C_1, C_2, C_3, σ_ϕ are constants for the $k-\varepsilon$ turbulent closure scheme. They are equal 1.44, 1.92, 1.0, 1.3 respectively. C_μ and $C_{\mu'}$ are calculated from the stability function.

As known, the equation fails in stably stratified flows, and for this reason almost all authors apply a clipping of the length scale as an ad hoc remedy. With this clipping, the

OSD
12, 2395–2421, 2015

maximum permissible length scale is determined by

$$l_{max} = C_{lim}\sqrt{2\bar{e}}/N. \tag{14}$$

A value of $C_{lim} = 0.53$ is often used (Galperin et al., 1988). Umlauf and Burchard (2005) show that the value of the clipping factor is of crucial importance for the entrainment depth predicted in stably stratified situations. Another value is 0.26, several authors have suggested limiting the dissipative length-scale in the presence of stable stratification even down to 0.07 (Holt and Umlauf, 2008).

In addition, convective mixing can be parameterized in NEMO by an enhancement to the eddy viscosity and diffusivity (ED), when for $N_2 < 0$, K_m and K_ρ are locally set to the value of $100\,\mathrm{m^2\,s^{-1}}$.

We performed comparative tests of listed above convection parameterizations to investigate their principal applicability for shear-induced convective situations.

3 Numerical experiments

The modeling period were chosen from 1 April to 31 August 2011 when pronounced thermocline occurs. The thermocline starts its formation in early May when the heating and turbulent mixing are dominant processes. Note that year 2011 was characterized by strong upwelling events in the beginning and in the end of modeling period.

In Sect. 2.1 the GLS, TKE and ED mixing parameterizations are compared in a series of sensitivity experiments. The choice of closure scheme and the effects of varying Galperin limit were investigated against MODIS SST to get the best reproduction of SST pattern.

In Sect. 2.2 we present results of the model runs compared with available CTD data to study the performance of the chosen parameterizations to represent the UML evolution. Also the ability of the model to correctly capture such features as fronts was tested against SST images for different resolutions in beginning of August 2011 when there were cloud free images.

OSD
12, 2395–2421, 2015

3.1 Sensitivity to vertical mixing parameterizations

In this section we study closure schemes and enhanced diffusion parameterization performance for convective situations caused by upwelling near the Estonian coast stated on 12 May. Figure 1 shows a cross section of the GOF for the density field (black isolines) overlaid by the vertical eddy diffusivity coefficient (color filled).

Fragment A of Fig. 1 illustrate the mechanism instability formation. It is a gipotertic solution obtained with constant eddy diffusivity coefficients set to the minimum possible for this case values of 10^{-4}–10^{-5} $m^2 c^{-1}$ and ED switched off. All cross-sections present the situation mainly formed by an upwelling event near the Estonian coast (left side of the cross-section). Due to the presence of permanent density gradient from Estonian to Finish coast and strong offshore current caused by upwelling, dense waters originated from the Estonian side overlay more fresh lighter water in the downwelling area near the Finish coast.

Fragment B illustrates the performance of the ED procedure setting the eddy viscosity and diffusivity coefficients equal to 100 $m^2 s^{-1}$ in the areas of unstable stratification. According to this experiment, the maximum depth of convection penetration is equal to 10 m in the center of GOF and reaches up to 25 m near the Finish coast.

Fragment C illustrates the performance of solution with the TKE closure scheme including previously described modifications introduced in NEMO. As seen, the solution demonstrates high values of eddy diffusion coefficients in the areas of unstable stratification. The depth of the mixed layer is not limited by the convection penetration depth (see Fig. 1b) and formed as a result of a joint action of current velocity shear, buoyancy and TKE diffusion and dissipation (see Eq. 1).

Fragment D shows the combined effect of cases B and C. As seen from comparison of Fig. 1d and c, the solution with modified TKE scheme captures most of the existing instabilities. ED (Fig. 1b) triggered only in some small areas in the center of the mixed layer and did not affect the actual mixing depth.

OSD
12, 2395–2421, 2015

Fragments E and F present the performance of the solution with the GLS closure scheme with Galperin limit of 0.53 and 0.26, correspondently. A solution with GLS parameterization with switched-off length scale limitation was also obtained but turned out to be practically equal to the case E. UML depth in these solutions is comparable to that in the cases C and D confirming success of TKE modifications in NEMO.

The above tests confirm that both TKE and GLS closure schemes used in NEMO are able to catch the convection induced by upwelling. As it comes from Fig. 1 an instability of vertical column initiates dramatic increasing in vertical diffusivity coefficients up to $0.04\,m^2\,s^{-1}$ TKE (Fig. 1c and d) or $0.036\,m^2\,s^{-1}$ GLS (Fig. 1e and f) from the background value set to $10^{-6}\,m^2\,s^{-1}$. TKE scheme forms a core with stronger mixing in the area of downwelling but at the same time the UML depth is comparable in both cases. Switched on ED do not modify UML depth predicted by turbulent closure schemes.

Evaluation of the actual performance of presented alternative parameterizations of convective processes is a complex task requiring high spatial and temporal resolution of in situ data that is not available at the moment. The sea surface temperature (SST) derived from the satellite thermal infrared imagery during cloud-free conditions provides significant information for monitoring of the relevant key ocean structures, such as fronts, eddies, and upwelling. At the same time, the SST fields can be used as an indicator of vertical mixing processes. As soon as we would get a realistic stratification, the surface pattern of simulated SST will also be in agreement with remotely observed SST.

Results of the comparison of modeled (various mixing parameterizations and resolutions) and MODIS-derived SST are presented at Fig. 2. The model shows that maximum upwelling development occurs on 14 May when the upwelling front reaches the center of the GOF and characterized by maximum temperature gradient across the front up to 5 °C. Unfortunately, due to heavy cloudiness, the satellite images captured only relaxation phase of the upwelling dated on 20 May.

As seen, the model performs better if the GLS scheme is used and the value of $C_{\rm lim}$ is 0.53 (Galperin's value). The stronger length scale limitation leads to underestimation

OSD
12, 2395–2421, 2015

of mixing and increased SST values compared to MODIS data. On the other hand, the solution obtained with TKE scheme underestimates mixing, nevertheless it is not too far from the observations. The best performance takes place at the higher resolution and GLS scheme used when the solution is in a good agreement with the MODIS SST (Fig. 2b). Based on presented sensitivity tests, the GLS mixing scheme was chosen and the length scale limiting was fixed as $C_{\text{lim}} = 0.53$

3.2 General model performance

To evaluate the general model performance, we used in situ data for temperature and salinity obtained during Russian state hydrometeorological institute expedition dated from 20 July 2011 to 5 August 2011. The comparison of model and data has been performed for the last decade of July just before the UML starts to degrade due to heating and wind conditions (Fig. 3). CTD data were grouped into three sets of profiles representing western (Lat 23:26, 10 profiles), central (Lat 26:28.2, 12 profiles) and eastern (Lat 28.2:30, 12 profiles) parts of the GOF. According to the presented at Fig. 3 averaged CTD profiles (black curves), the UML is much deeper in the western part of the GOF and considerably shallower and sharper in the central and eastern parts. This UML behavior typical for the GOF captured quite well by all the model realizations (colored curves). Standard deviation of CTD data given as error bars presents the variability corridor of in situ data. All presented solutions with different parameterizations are in good agreement with the data in terms of the UML depth while the fine spatial resolution slightly better represents the nature in the western part of GOF. In the eastern part of GOF strongly influenced by the Neva outflow the modeled thermocline is about 5 m deeper than observed. This is mainly due to prescribing climatic boundary conditions at the river mouth not allowing for the differences in individual years and complicated hydrodynamics of the estuary.

One more comparison between model and data is presented in Fig. 4 where the modeled SST for the two resolutions is given vs. MODIS SST on 2 August 2011. At this time it was possible to fix the upwelling again near the southern coast of GOF. In the

OSD
12, 2395–2421, 2015

high resolution model solution the temperature of cold water rising to the surface drops down to 6 °C that is consistent with the satellite SST. In the case of coarse resolution the upwelling effect is less pronounced: the lowest temperature in the core region is about 10 °C. Solutions with both resolutions reproduce spatial patterns of upwelling. Although the coarse resolution solution gives more flattened upwelling front (shown by the isotherm of 19.5 °C), high resolution solution is more rugged due to reproduced submesoscale features that corresponds well with observed SST.

Results of model comparison with SST and in situ data confirm the robustness of the developed model, which allows us to use it in a more detailed evaluation of the vertical structure formation mechanisms of the sea and it's temporal evolution.

4 Results

During the upwelling/downwelling event in May model on both grids simulates a substantial re-stratification of the UML. The re-stratification is characterized by sharpening and at the same time deepening of the thermocline down to 40 m near the Finish coast and export of the cold water to the surface near the Estonian coast (Fig. 5). Figure 5a and b shows maps of the turbocline depth on the 16 May 2011. The turbocline depth is defined as the depth at which the vertical eddy diffusivity coefficient falls below a given value (here taken equal to background value of 5 $cm^2 s^{-1}$) and can be interpreted as a maximum penetration depth of the turbulent motion in the surface layer.

According to Fig. 5a and b presenting solutions on 2 and 0.5 km grids correspondently, the turbocline depth reaches the maximum in the areas near the Finnish coast where the convection is a dominant factor in vertical mixing. We can note the significant differences in the spatial patterns of the turbocline for fine and rough resolutions. Solution on 0.5 km grid shows deeper and more complex thermocline paten. It can be explained by the fact that small-scale frontal structures induced by strong horizontal gradients and captured by the fine model lead to convective instabilities (Boccaletti et al.,

2007) acting to locally restratify UML. The model with 2 km resolution cannot resolve submesoscale frontal features and high values (compare to fine resolution) of lateral diffusion coefficients act to smooth the front in other words decreasing potential energy of the front. Unfortunately, few data is available for validation of these differences. Locations of CTD profiles on 16 May are marked as points I, II, III in Fig. 5a and c. However, the UML depth for the 2 km model are not deep enough, barely reaching 25 m depth everywhere whereas observations in western part show it values reaching a maximum of about 40 m depth.

Figure 6 presents evolution of the thermocline through the season. Left panels present the maximum depth of the turbolcline and thermocline for the May when the thermocline was formed. Right panels present also maximum turbolcline and thermocline depths but for the period from 1 June to 28 July. This period ends just before the upwelling in July–August from which the UML erosion begins. Thermocline depth was defined as the depth of 3.5 °C isotherm (see Fig. 3). As it comes from the presented data, turbulent mixing during the upwelling in May was the strongest throughout the season (see Fig. 6b). At the same time increasing of the 3.5 °C isotherm depth up to 45 m during June–July is not accomplished by any considerable turbulent activity (maximum turbocline depth during June–July do not exceed 20 m for the most of the territory of the GOF). Taking in consideration the low value of the background vertical diffusivity coefficient (10^{-6} m^2 s^{-1}), this fact highlights the importance of the advective processes for the formation of the shape and depth of the thermocline. Advective processes resulting in deepening of the isotherm are initiated by intrusion of warm dense water from the open boundary from the Baltic Proper. The intrusion compensates the general surface outflow from the GOF caused by rivers runoff. Notable difference in the shape of averaged profiles presented at Fig. 3 confirm this hypothesis. Eastern part of the GOF characterized by sharp and shallow thermocline and halocline. Their depths are approximately equal to the maximum turbocline depth. Turbulent and heating processes are dominated here. Deepening of the thermocline and halocline down

OSD
12, 2395–2421, 2015

to 45 m in the western part of GOF is caused mainly by the GOF-Baltic Sea exchange processes since turbulent mixing do not penetrate at this depth here.

The sensitivity of the model solution to increased horizontal resolution manifested in the different intrusion propagation to east (compare right plots on Fig. 6d and f). Density fronts associated with the intrusion are a source of baroclinic instability which are differently resolved by the 0.5 km eddy permitting configuration (Fig. 6c) compared to 2 km configuration (Fig. 6e).

5 Discussion and conclusions

We used state-of-the-art modeling framework NEMO initially developed for the open ocean to build an eddy resolving model of the GOF. To evaluate the model skill and performance two different solutions where obtained: commonly used 2 km grid and 0.5 km eddy resolving fine grid. Refinement below this level at shelf scale would be of limited benefit in a hydrostatic model. Increased model resolution was found to better capture the position and strength of the SST front. Moreover, instabilities along the front led to large temporal and spatial variability of UML in the high resolution model. The role of submesoscale flows in setting stratification in the upper ocean over the annual cycle has been investigated.

Hydrostatic hypothesis removes convective processes from the initial Navier–Stokes equations and so convective processes must be parameterized instead. In this study we used available in NEMO parameterizations of convective processes to reproduce the interaction of small-scale baroclinic instabilities with turbulent mixing in the frame of the hydrostatic assumption. We explore the efficacy of convection parameterizations available in NEMO and found that GLS or even modified TKE closure schemes can describe convective processes in UML of GOF without additional convective adjustment procedures.

It is found that simulations which resolve submesoscale are characterized by the deeper UML with more complex structure in the regions of the GOF directly affected

OSD
12, 2395–2421, 2015

by the upwelling/downwelling. It is noteworthy that data coverage may not be enough to outline the differences in behavior of the model resolutions.

Increasing of resolution also leads to an increase in the propagation distance of intrusions from the Baltic Proper. This fact should be deeply investigated by excluding of possible boundary effects: for example, through a shift of the open boundary to the west or running the model for entire Baltic Sea.

Since the time period of the runs was rather short (less than 1 year) and the model had not been used before it is obvious that choose of some parameters might have been somewhat improper for the use in this study. Through fine tuning of the model better results could be probably obtained. However, the focus in this study was to examine the differences arising from different horizontal resolutions, the fact that model parameters were similar in each case should be considered to be far more important than the quantitative agreement between observations and model results. Actually, it was shown that the model results for both resolutions are in a reasonable agreement with available observations.

It has been clearly demonstrated that a combined analysis of observations, in our case of remote sensing data, and the results of numerical modeling, is superior to single methods alone in many ways. The usage of results of hydrodynamic modeling together with SST information can provide an extended analysis and deeper understanding of the upwelling process. Convection induced by upwelling in the surface layer promotes to re-stratification of the UML and results in changes of the SST pattern observed from satellites. Lateral movements induced by upwelling lead to considerable re-stratification of the GOF. Our results unambiguously suggest the occurrence of shear-induced convection in stratified waters of GOF which is characterized by presence of permanent lateral density gradient in the north–south direction. This is a potentially important mixing mechanism that has yet to be explored in detail in this context and hence deserves further investigation.

It should be emphasized that the model captures principal difference in the thermocline and halocline shape for the western and eastern parts of GOF. Adequate rep-

OSD
12, 2395–2421, 2015

resentation of lateral processes by the model let us decrease the role of background constants in turbulent mixing scheme. This simplifies the traditional trade-off between the depth and sharpness of the thermocline. Setting the background values of vertical eddy viscosity and diffusivity to 10^{-5} and 10^{-7} correspondently let us keep the sharp form of the thermocline and halocline while UML depth corresponds to observations. Most of the mixing is achieved by the wind and convective processes caused by upwelling and intrusions. This approach demonstrates a substantial improvement in the modeled basin stratification compared to previous numerical studies.

Acknowledgements. This work was supported by the Federal Targeted Programme for Research and Development in Priority Areas of Development of the Russian Scientific and Technological Complex for 2014–2020 (Grant Agreement No.: RFMEFI57414X0091).

References

Alenius, P., Myrberg, K., and Nekrasov, A.: The physical oceanography of the Gulf of Finland: a review, Boreal Environ. Res., 3, 97–125, 1998.

Alenius, P., Nekrasov, A., and Myrberg, K.: The baroclinic Rossby-radius in the Gulf of Finland, Cont. Shelf Res., 23, 563–573, 2003.

Andrejev, O., Sokolov, A., Soomere, T., Värv, R., and Viikmäe, B.: The use of high-resolution bathymetry for circulation modelling in the Gulf of Finland, Estonian Journal of Engineering, 16, 187–210, 2010.

Boccaletti, G., Ferrari, R., and Fox-Kemper, B.: Mixed layer instabilities and restratification, J. Phys. Oceanogr., 37, 2228–2250, 2007.

Bougeault, P. and Lacarrère, P.: Parameterization of orography-induced turbulence in a mesobeta-scale model, Mon. Weather Rev., 117, 1872–1890, 1989.

Funkquist, L.: HIROMB, an operational eddy-resolving model for the Baltic Sea, Bulletin of the Maritime Institute in Gdansk, XXVIII, 7–16, 2001.

Galperin, B., Kantha, L. H., Hassid, S., and Rosati, A.: A quasi-equilibrium turbulent energy model for geophysical flows, J. Atmos. Sci., 45, 55–62, 1988.

Gaspar, P., Gregoris, Y., and Lefevre, J.-M.: A simple eddy kinetic energy model for simulations of the oceanic vertical mixing: Tests at station Papa and long-term upper ocean study site, J. Geophys. Res., 95, 16179–16193, 1990.
Gent, P. R. and McWilliams, J. C.: Isopycnal mixing in ocean circulation models, J. Phys. Oceanogr., 20, 150–155, 1990.
Hankimo, J.: Some computations of the energy exchange between the sea and the atmosphere in the Baltic area, Finnish Meteorological Office Contributions, 57, 26 pp., 1964.
High Resolution Limited Area Modelling project HIRLAM: available at: http://hirlam.org, last access: 1 February 2015.
Holt, J. and Umlauf, L.: Modelling the tidal mixing fronts and seasonal stratification of the Northwest European Continental Shelf, Cont. Shelf Res., 28, 887–903, 2008.
Kantha, L. H. and Clayson, C. A.: An improved mixed layer model for geophysical applications, J. Geophys. Res., 99, 25235–25266, 1994.
Kolmogorov, A. N.: The equation of turbulent motion in an incompressible fluid, Izvestiya Akademii Nauk SSSR Seriya Fizicheskaya, 6, 56–58, 1942.
Laine, A. O., Andersin, A.-B., Leinio, S., and Zuur, A. F.: Stratification-induced hypoxia as a structuring factor of macrozoobenthos in the open Gulf of Finland (Baltic Sea), J. Sea Res., 57, 65–77, 2007.
Lips, U., Lips, I., Liblik, T., and Elken, J.: Estuarine transport versus vertical movement and mixing of water masses in the Gulf of Finland (Baltic Sea), in: US/EU-Baltic International Simposium, 2008 IEEE/OES, 1–8, doi:10.1109/BALTIC.2008.4625535, Tallinn, 27–29 May 2008.
Lips, U., Lips, I., Liblik, T., and Kuvaldina, N.: Processes responsible for the formation and maintenance of sub-surface chlorophyll maxima in the Gulf of Finland, Estuar. Coast Shelf S., 88, 339–349, 2010.
Liu, H. and Holt, J. T.: Combination of the Vertical PPM Advection Scheme with the Existing Horizontal Advection Schemes in NEMO, MyOcean Science Days, available at: http://mercator-myoceanv2.netaktiv.com/MSD2010/Abstract/AbstractLIUhedongMSD2010.doc (last access: 1 June 2013), 2010.
Lorke, A., Peeters, F., and Wuëst, A.: Shear-induced convective mixing in bottom boundary layers on slopes, Limnol. Oceanogr., 50, 1612–1619, 2005.
Madec, G.: NEMO ocean engine. Note du Pôle de modélisation, Institut Pierre-Simon Laplace (IPSL), Paris, France, No 27 ISSN No 1288–1619, 2012.

OSD
12, 2395–2421, 2015

Effects of lateral processes on the seasonal water stratification of the Gulf of Finland

R. E. Vankevich et al.

Madec, G., Delecluse, P., Imbard, M., and Levy, C.: OPA 8.1 Ocean General Circulation Model reference manual. Note du Pole de modelisation, Institut Pierre-Simon Laplace (IPSL), Paris, France, No 11, 91 p., 1998.

Maximov, A. A.: Causes of the bottom hypoxia in the eastern part of the Gulf of Finland in the Baltic Sea, Oceanology, 46, 204–210, 2006.

Mellor, G. L. and Yamada, T.: A hierarchy of turbulence closure models for planetary boundary layers, J. Atmos. Sci., 31, 1791–1806, 1974.

Myrberg, K., Ryabchenko, V., Isaev, A., Vankevich, R., Andrejev, O., Bendtsen, J., Erichsen, A., Funkquist, L., Inkala, A., Neelov, I., Rasmus, K., Medina, M. R., Raudsepp, U., Passenko, J., Soderkvist, J., Sokolov, A., Kuosa, H., Anderson, T. R., Lehmann, A., and Skogen, M. D.: Validation of three-dimensional hydrodynamic models of the Gulf of Finland, Boreal Environ. Res., 15, 453–479, 2010.

Nekrasov, A. V. and Lebedeva, I. K.: Estimation of baroclinic Rossby radius Koporye region, BFU Research Bulletin, 4–5, 89–93, 2002.

Rantajarvi, E., Gran, V., Hällfors, S., and Olsonen, R.: Effects of environmental factors on the phytoplankton community in the Gulf of Finland – unattended high frequency measurements and multivariate analyses, Hydrobiologia, 363, 127–139, 1998.

Rippeth, T. P., Fisher, N. R., and Simpson, J. H.: The cycle of turbulent dissipation in the presence of tidal straining, J. Phys. Oceanogr., 31, 2458–2471, 2001.

Rodi, W.: Examples of calculation methods for flow and mixing in stratified Fluids, J. Geophys. Res., 92, 5305–5328, 1987.

Sokolov, A.: Modelling of submesoscale dynamics in the Gulf of Finland (Baltic Sea), Geophysical Research Abstracts Vol. 15, EGU2013–9646, General Assembly, Vienna, Austria, 2013.

Soomere, T., Myrberg, K., Leppäranta M., and Nekrasov, A.: The progress in knowledge of physical oceanography of the Gulf of Finland: a review for 1997–2007, Oceanologia, 50, 287–362, 2008.

Soomere, T., Leppäranta M., and Myrberg, K.: Highlights of the physical oceanography of the Gulf of Finland reflecting potential climate changes, Boreal Environ. Res., 14, 152–165, 2009.

Stalnacke, P., Grimvall, A., Sundblad, K., and Tonderski, A.: Estimation of riverine loads of nitrogen and phosphorus to the Baltic Sea 1970–1993, Environ. Monit. Assess., 58, 173–200, 1999.

OSD
12, 2395–2421, 2015
Effects of lateral processes on the seasonal water stratification of the Gulf of Finland
R. E. Vankevich et al.

Stepputtis, D., Hinrichsen, H.-H., Bottcher, U., Gotze, E., and Mohrholz, V.: An example of meso-scale hydrographic features in the central Baltic Sea and their influence on the distribution and vertical migration of sprat, *Sprattus sprattus balticus* (Schn.), Fish. Oceanogr., 20, 82–88, 2011.
Thomas, L., Tandon, A., and Mahadevan, A.: Submesoscale ocean processes and dynamics, in: Ocean Modeling in an Eddying Regime, edited by: Hecht, M. and Hasume, H., Geophysical Monograph 177, American Geophysical Union, Washington DC, 217–228, 2007.
Tuomi, L., Myrberg, K., and Lehmann, A.: The performance of different vertical turbulence parameterizations in modelling the development of the seasonal thermocline in the Gulf of Finland, Geophysical Research Abstracts Vol. 15, EGU2013-8229, General Assembly, Vienna, Austria, 2013.
Umlauf, L.: Modelling the effects of horizontal and vertical shear in stratified turbulent flows, Deep-Sea Res. Pt. II, 52, 1181–201, 2005.
Umlauf, L. and Burchard, H.: A generic length-scale equation for geophysical turbulence models, J. Marine Syst., 61, 235–265, 2003.
Umlauf, L. and Burchard, H.: Second-order turbulence closure models for geophysical boundary layers, a review of recent work, J. Marine Syst., 25, 795–827, 2005.
Zhurbas, V., Laanemets, J., and Vahtera, E.: Modeling of the mesoscale structure of coupled upwelling/downwelling events and the related input of nutrients to the upper mixed layer in the Gulf of Finland, Baltic Sea, J. Geophys. Res., 113, C05004, doi:10.1029/2007JC004280, 2008.

OSD
12, 2395–2421, 2015

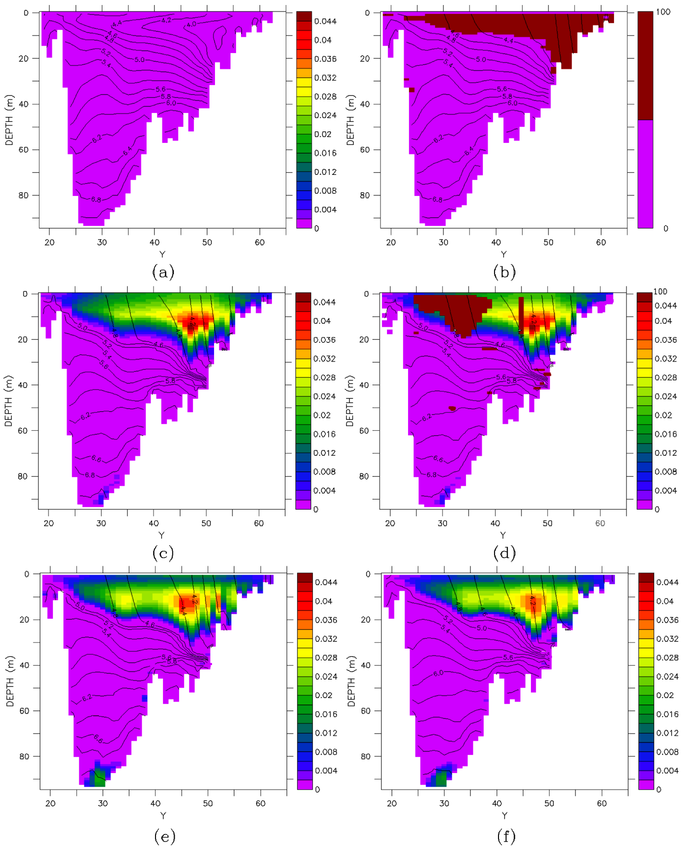

Figure 1. Meridional cross section of the GOF at 25.5° E. Vertical eddy diffusivity coefficient (shaded surface) overlaid by density isolines: **(a)** constant vertical eddy viscosity/diffusivity coefficients set to the $10^{-4}/10^{-5}\,m^2\,s^{-1}$, **(b)** convective adjustment only (ED), **(c)** TKE, **(d)** TKE + ED, **(e)** GLS with Galperin limit set to 0.53, **(f)** GLS with Galperin limit set to 0.26.

OSD
12, 2395–2421, 2015

Effects of lateral processes on the seasonal water stratification of the Gulf of Finland

R. E. Vankevich et al.

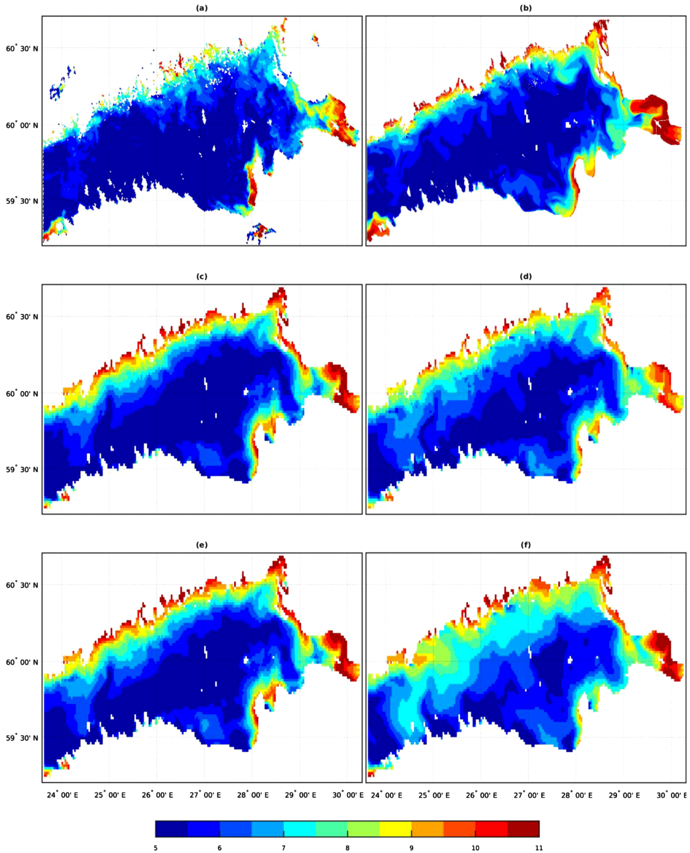

Figure 2. SST on 20 May 2011: **(a)** MODIS SST, **(b)** GLS with Galperin limit 0.53 and horizontal resolution 0.5 km, **(c)** GLS with Galperin limit 0.53 and horizontal resolution 2 km, **(d)** GLS with Galperin limit 0.26 and horizontal resolution 2 km, **(e)** TKE with convective adjustment and horizontal resolution 2 km, **(f)** GLS with Galperin limit 0.07 and horizontal resolution 2 km.

OSD
12, 2395–2421, 2015

Effects of lateral processes on the seasonal water stratification of the Gulf of Finland

R. E. Vankevich et al.

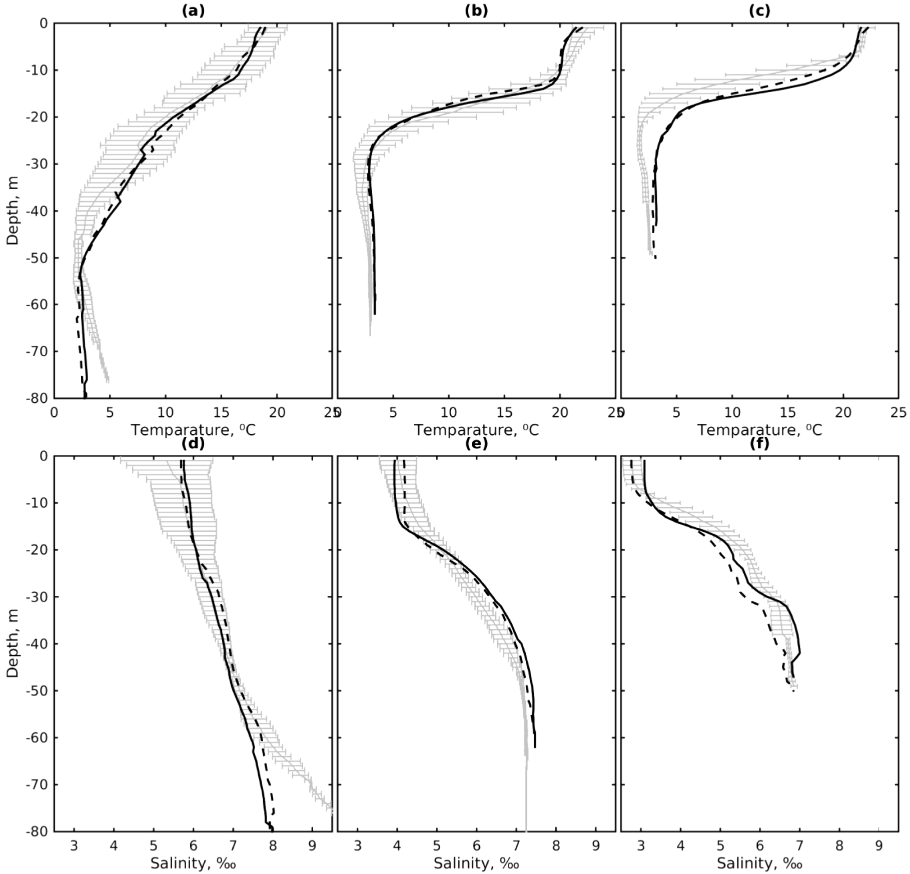

Figure 3. Averaged vertical profiles of temperature and salinity in west **(a, d)**, central **(b, e)** and east **(c, f)** parts of GOF for the period 20 July–5 August 2011. Grey lines – CTD data with standard deviation corridors, solid and dashed black lines – model on grids 0.5 and 2 km correspondently.

OSD
12, 2395–2421, 2015

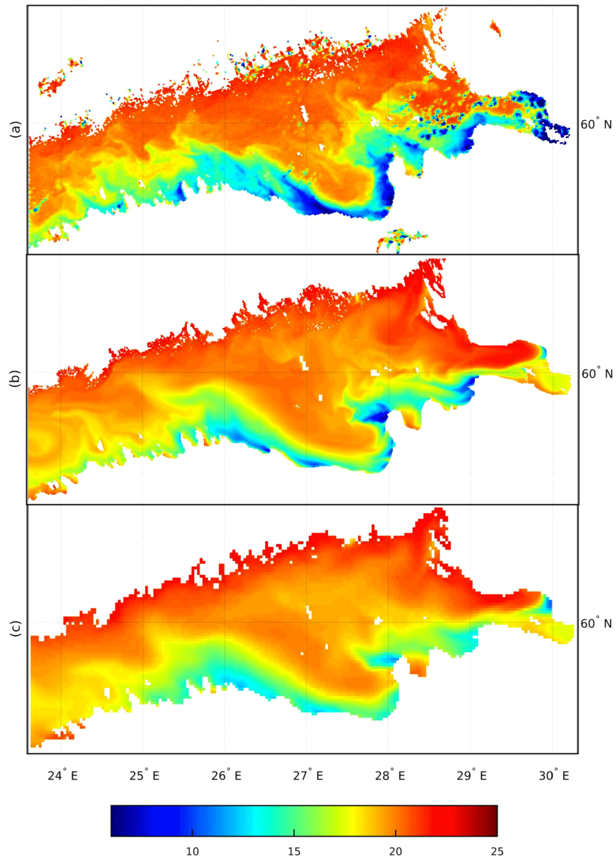

Figure 4. SST maps of GOF on 2 August 2011: **(a)** MODIS data, (**b** and **c**) modeled SST on grids 0.5 and 2 km correspondently.

OSD
12, 2395–2421, 2015

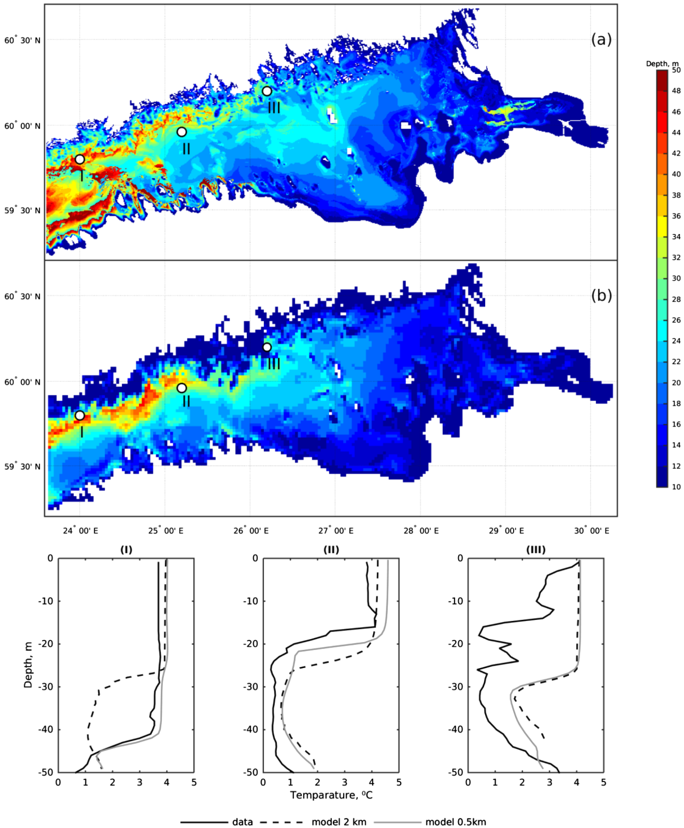

Figure 5. Modelled turbocline depth (m) in GOF on 20 May 2011: (**a** and **b**) horizontal distributions on grids 0.5 and 2 km correspondently; (I), (II) and (III) – vertical profiles of temperature at the locations marked on maps (**a** and **b**).

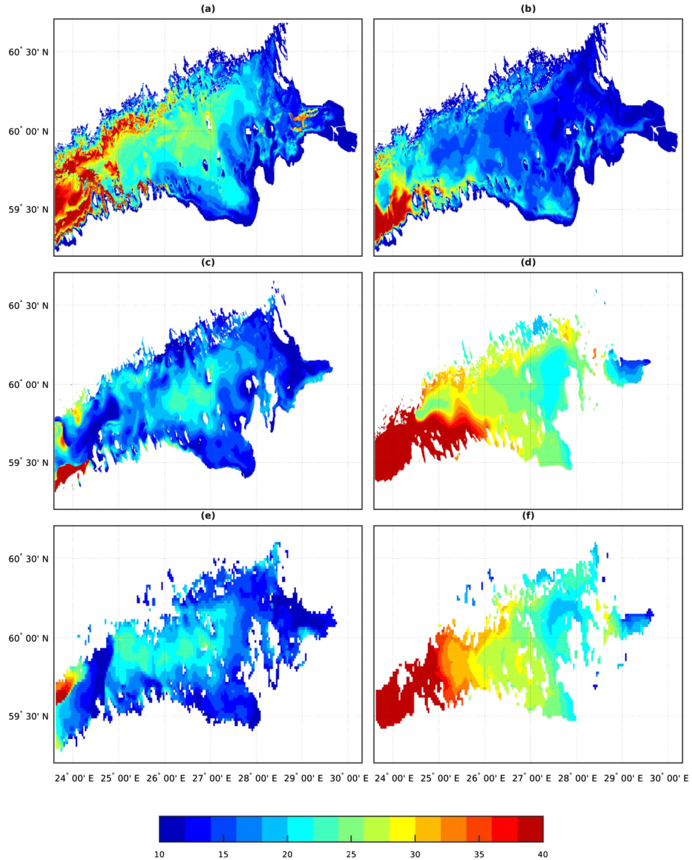

Figure 6. Depth of isotherm 3.5 °C and turbocline depth for the periods: left column 11–30 May 2011, right column 20–28 July 2011. **(a, b)** – maximum turbocline depth, model 0.5 km resolution, **(c, d)** – isotherm 3.5 °C depth model 0.5 km; **(e, f)** – isotherm 3.5 °C depth model 2 km.

OSD
12, 2395–2421, 2015

Effects of lateral processes on the seasonal water stratification of the Gulf of Finland

R. E. Vankevich et al.